

Interacting plasmon and phonon polaritons in aligned nano- and microwires

Viktor Myroshnychenko,^{1,*} Andrzej Stefanski,² Alejandro Manjavacas,¹ Maria Kafesaki,³ Rosa I. Merino,⁴ Victor M. Orera,⁴ Dorota Anna Pawlak,² and F. Javier García de Abajo^{1,5}

¹*Instituto de Química-Física "Rocasolano" - CSIC, Serrano 119, 28006 Madrid, Spain*

²*Institute of Electronic Materials Technology, Wólczyńska 133, 01-919 Warsaw, Poland*

³*Institute of Electronic Structure and Laser Foundation for Research and Technology Hellas, University of Crete, Heraklion, Crete, Greece*

⁴*Instituto de Ciencia de Materiales de Aragón (Universidad de Zaragoza-CSIC), Facultad de Ciencias, Pedro Cerbuna 12, Zaragoza E-50009, Spain*

⁵*J.G.deAbajo@csic.es*

[*v.myroshnychenko@csic.es](mailto:v.myroshnychenko@csic.es)

Abstract: The availability of macroscopic, nearly periodic structures known as eutectics opens a new path for controlling light at wavelength scales determined by the geometrical parameters of these materials and the intrinsic properties of their component phases. Here, we analyze the optical waveguiding properties of eutectic mixtures of alkali halides, formed by close-packed arrangements of aligned cylindrical inclusions. The wavelengths of phonon polaritons in these constituents are conveniently situated in the infrared and are slightly larger than the diameter and separation of the inclusions, typically consisting on single-crystal wires down to submicrometer diameter. We first discuss the gap mode and the guiding properties of metallic cylindrical waveguides in the visible and near-infrared, and in particular we investigate the transition between cylinder touching and non-touching regimes. Then, we demonstrate that these properties can be extended to the mid infrared by means of phonon polaritons. Finally, we analyze the guiding properties of an actual eutectic. For typical eutectic dimensions, we conclude that crosstalk between neighboring cylindrical wires is small, thus providing a promising platform for signal propagation and image analysis in the mid infrared.

© 2012 Optical Society of America

OCIS codes: (250.5403) Plasmonics; (240.6680) Surface plasmons; (230.7370) Waveguides.

References and links

1. M. Quinten, A. Leitner, J. R. Krenn, and F. R. Aussenegg, "Electromagnetic energy transport via linear chains of silver nanoparticles," *Opt. Lett.* **23**, 1331–1333 (1998).
2. S. A. Maier, M. L. Brongersma, P. G. Kik, S. Meltzer, A. A. G. Requicha, and H. A. Atwater, "Plasmonics - a route to nanoscale optical devices," *Adv. Mater.* **13**, 1501–1505 (2001).
3. S. I. Bozhevolnyi, V. S. Volkov, E. Devaux, J. Y. Laluet, and T. W. Ebbesen, "Channel plasmon subwavelength waveguide components including interferometers and ring resonators," *Nature* **440**, 508–511 (2006).
4. E. Moreno, S. G. Rodrigo, S. I. Bozhevolnyi, L. Martín-Moreno, and F. J. García-Vidal, "Guiding and focusing of electromagnetic fields with wedge plasmon polaritons," *Phys. Rev. Lett.* **100**, 023901 (2008).

5. R. F. Oulton, V. J. Sorger, D. A. Genov, D. F. P. Pile, and X. Zhang, "A hybrid plasmonic waveguide for sub-wavelength confinement and long-range propagation," *Nat. Photonics* **2**, 496–500 (2008).
6. A. Manjavacas and F. J. García de Abajo, "Robust plasmon waveguides in strongly interacting nanowire arrays," *Nano Lett.* **9**, 1285–1289 (2009).
7. A. Manjavacas and F. J. García de Abajo, "Coupling of gap plasmons in multi-wire waveguides," *Opt. Express* **17**, 19401–19413 (2009).
8. J. A. Conway, S. Sahni, and T. Szkopek, "Plasmonic interconnects versus conventional interconnects: A comparison of latency, crosstalk and energy costs," *Opt. Express* **15**, 4474–4484 (2007).
9. A. J. Huber, B. Deutsch, L. Novotny, and R. Hillenbrand, "Focusing of surface phonon polaritons," *Appl. Phys. Lett.* **92**, 203104 (2008).
10. N. W. Ashcroft and N. D. Mermin, *Solid State Physics* (Harcourt College Publishers, New York, 1976).
11. J. S. Kirkaldy, "Predicting the patterns in lamellar growth," *Phys. Rev. B* **30**, 6889–6895 (1984).
12. J. Llorca and V. M. Orera, "Directionally-solidified eutectic ceramic oxides," *Prog. Mat. Sci.* **51**, 711–809 (2006).
13. D. A. Pawlak, G. Lerondel, I. Dmytruk, Y. Kagamitani, S. Durbin, and T. Fukuda, "Second order self-organized pattern of terbium-scandium-aluminum garnet and terbium-scandium perovskite eutectic," *J. Appl. Phys.* **91**, 9731–9736 (2002).
14. D. A. Pawlak, K. Kolodziejek, S. Turczynski, J. Kisielewski, K. Rozniatowski, R. Diduszko, M. Kaczkan, and M. Malinowski, "Self-organized, rodlike, micrometer-scale microstructure of $Tb_3Sc_2Al_3O_{12}$ - $TbScO_3$:Pr eutectic," *Chem. Mater.* **18**, 2450–2457 (2006).
15. D. A. Pawlak, S. Turczynski, M. Gajc, K. Kolodziejek, R. Diduszko, K. Rozniatowski, J. Smalc, and I. Vendik, "How far are we from making metamaterials by self-organization? The microstructure of highly anisotropic particles with an SRR-like geometry," *Adv. Funct. Mat.* **20**, 1116–1124 (2010).
16. A. Larrea, L. Contreras, R. I. Merino, J. Llorca, and V. M. Orera, "Microstructure and physical properties of CaF_2 - MgO eutectics produced by the Bridgman method," *J. Mater. Res.* **15**, 1314–1319 (2000).
17. F. J. García de Abajo and A. Howie, "Relativistic electron energy loss and electron-induced photon emission in inhomogeneous dielectrics," *Phys. Rev. Lett.* **80**, 5180–5183 (1998).
18. F. J. García de Abajo and A. Howie, "Retarded field calculation of electron energy loss in inhomogeneous dielectrics," *Phys. Rev. B* **65**, 115418 (2002).
19. F. J. García de Abajo, A. G. Pattantyus-Abraham, N. Zabala, A. Rivacoba, M. O. Wolf, and P. M. Echenique, "Cherenkov effect as a probe of photonic nanostructures," *Phys. Rev. Lett.* **91**, 143902 (2003).
20. E. D. Palik, *Handbook of Optical Constants of Solids* (Academic Press, San Diego, 1985).
21. I. Romero, J. Aizpurua, G. W. Bryant, and F. J. García de Abajo, "Plasmons in nearly touching metallic nanoparticles: Singular response in the limit of touching dimers," *Opt. Express* **14**, 9988–9999 (2006).
22. J. P. Kottmann and O. J. F. Martin, "Plasmon resonant coupling in metallic nanowires," *Opt. Express* **8**, 655–663 (2001).
23. V. M. Orera and A. Larrea, "NaCl-assisted growth of micrometer-wide long single crystalline fluoride fibres," *Opt. Mater.* **27**, 1726–1729 (2005).
24. P. A. Belov and Y. Hao, "Subwavelength imaging at optical frequencies using a transmission device formed by a periodic layered metal-dielectric structure operating in the canalization regime," *Phys. Rev. B* **73**, 113110 (2006).

1. Introduction

Optical waveguiding constitutes a pillar stone of photonic devices for light signal processing. In recent years, several strategies have been followed to gain further control over guiding at the nano- and microscales, taking advantage of the growing degree of understanding of plasmons, on which several well-known designs are relying. More precisely, waveguiding has been demonstrated to take place due to hopping of localized plasmons between neighboring particles in linear arrays [1, 2]. Propagating plasmon waveguides have been explored based upon channel and ridge structures patterned on metal surfaces [3, 4]. Hybrid structures consisting of metallodielectric elements have also been proposed [5]. A particularly promising geometry is the nanowire pair, which offers a record level of integrability in three dimensions [6, 7]. Plasmons confined within the gap between two neighboring aligned nanowires can travel over relatively large distances without excessively protruding outside the gap region, thus minimizing the risk of crosstalk with other neighboring structures, which is an issue to be considered when contemplating plasmon waveguides [8].

A similar strategy can be used for other excitations within the electromagnetic spectrum. For instance, focusing near-field imaging [9] of phonon polaritons has been achieved in SiC

at $\sim 10\mu\text{m}$ wavelength. At even longer wavelengths, optical phonons in alkali-halide crystals display a dielectric behavior in the mid infrared similar to plasmons in the visible and near infrared (i.e., optical metallic performance, characterized by large negative permittivities and small losses). The origin of these resonances lies in the optical phonons supported by these materials [10]. We thus expect that optical-phonon polaritons can undergo a waveguiding behavior similar to plasmons, which can be advantageous to handle infrared light and contribute to ease the lack of suitable devices in this regime.

In this context, eutectics emerge as ideal systems to fabricate relatively large-scale structures containing repeated patterns with added optical functionalities, and in particular, wire-based eutectics exhibit typical patterns mimicking two-dimensional photonic crystals formed by hexagonal arrangements of aligned wires. Eutectics are structured composites made of two immiscible component phases, which are self-organized into nearly regular patterns when they solidify under controlled growth conditions [11, 12]. Various component materials can be used for eutectic creation, leading to varied geometries with different functionalities. Actually, eutectics solidification has been already proposed as a potential way of manufacturing photonic crystals [13] and metamaterials [14, 15]. Eutectics can be prepared with a controlled precipitate size from micrometers down to tens of nanometers [14]. Interestingly, alkali-halide eutectics can be prepared with wire diameters and separations of only a few microns and containing hundreds of thousands of single crystalline wires aligned into a dielectric matrix [16]. These dimensions are comparable to or smaller than the infrared wavelength of their polaritonic excitations. Therefore, eutectics provide a promising path to the design of extended structures that support waveguiding of optical-phonon polaritons in the infrared regime.

In this paper, we study optical waveguiding in aligned nano- and microwires. Specifically, we investigate gap guided modes in neighboring silver nanowires and the evolution of these modes in separate and overlapping wires near the transition between touching and non-touching regimes. We then show that similar gap modes are indeed trapped by neighboring alkali-halide microwires. The guiding properties of these modes are studied in detail for an actual system consisting of LiF wires embedded in NaCl. Gap modes are found to interact very weakly with other structures far from the gap. The propagation distance depends critically on the separation between neighboring wires. Our study is based upon rigorous solution of the Maxwell equations via two different methods: (1) a two-dimensional version of the boundary element method (BEM) [17, 18] to simulate the local density of optical states (LDOS) and the near-field intensities; and (2) a multiple-scattering approach to find the total density of states in finite arrangements of non-overlapping wires [19]. We achieve convergence using ~ 100 parametrization points per wire in BEM and ~ 10 two-dimensional multipoles per wire in the multiple-scattering method. The dielectric functions of the materials considered here are taken from optical data [20]. The translational symmetry of the problem permits studying guided modes as a function of their frequency ω and wave vector parallel to the wires k_{\parallel} . An overall dependence of the fields on time t and distance along the wires z as $\exp(ik_{\parallel}z - i\omega t)$ is thus understood.

2. Gap plasmons in silver nanowire pairs

We first consider gap plasmons in silver nanowires. Figure 1 analyzes the evolution of these plasmons with the separation between wires. For the dimensions under consideration and for fixed value of k_{\parallel} , we observe a low energy mode in the LDOS at the center of the wire pair. This is the gap plasmon. As the separation is decreased, the mode is increasingly more confined (this conclusion is supported by the spatial distribution of the LDOS for various separations, see Fig. 1(c)), and it migrates towards lower energy (Fig. 1(b)). Such redshifts are familiar in the plasmons of particle dimers [21]. Incidentally, these gap plasmons involve monopoles of opposite signs in the wires [6, 22]. Charge neutrality within each wire is then preserved by the

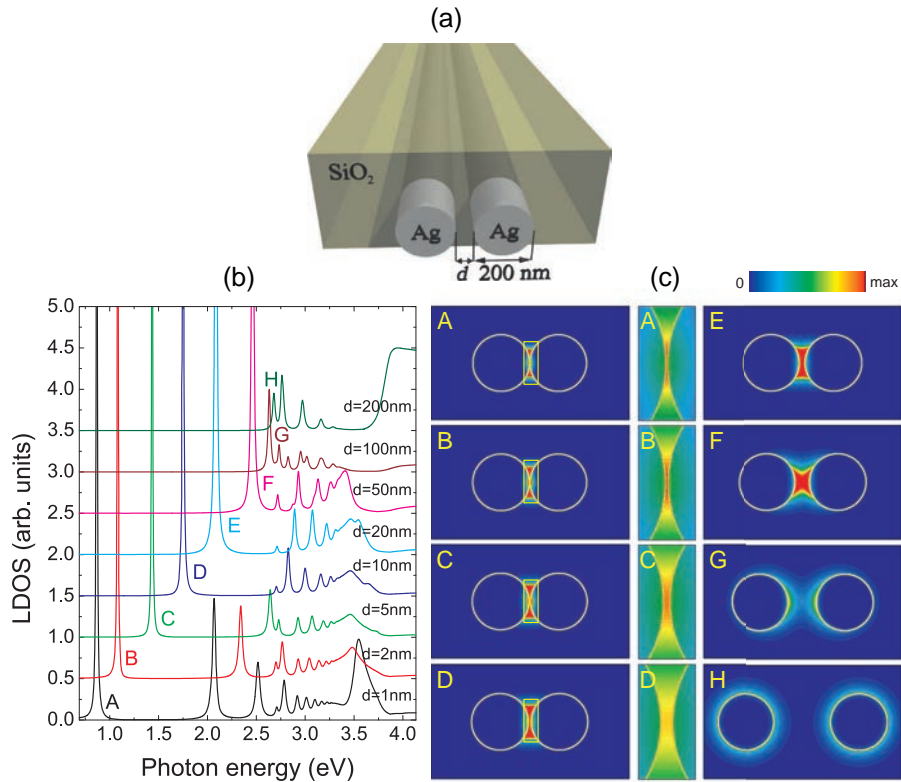


Fig. 1. Gap plasmons of aligned silver nanowires in silica: non-touching configuration. **(a)** Schematic view of the geometry. The wires have a diameter of 200 nm and their separation varies from 1 nm to 200 nm. **(b)** Spectral dependence of the local density of photonic states (LDOS) at the gap center for fixed parallel wave vector $k_{\parallel} = 27 \mu\text{m}^{-1}$ along the wire axes. **(c)** Spatial distribution of the LDOS for the low-energy gap modes. Zooms of the gap region of plots A-D are shown as well. The color scale is normalized to the intensity maximum for each separation.

periodic oscillation of the modes along z as $\exp(ik_{\parallel}z)$.

When the wires overlap, a mode is observed that is confined within the junction. Interestingly, this mode is rather insensitive to the actual overlap between wires for $|d| < 10\text{nm}$, in contrast to what is observed in particle dimers [21]. If the degree of overlap is sufficiently large, the junction mode disappears, and the LDOS spectra (Fig. 2(b)) slowly converge towards the individual wire. The degree of confinement of the junction mode is significant, although it is low compared to the gap mode for similar values of the separation $|d|$ around the touching limit $d = 0$.

A more complete picture of gap and junction plasmons is presented in Fig. 3, which shows dispersion diagrams of the LDOS as a function of k_{\parallel} and ω for a wide range of separations from touching ($d < 0$) to non-touching ($d > 0$) regimes, with emphasis in the near-touching limit ($d = 0$). The gap mode is indeed evolving towards the red with decreasing separations between non-touching wires. This behavior is clearly leading to increasing separation from the light cone, which is consistent with the observed larger degree of confinement. For $k_{\parallel} > k_{\text{silica}}$ outside the light cone of silica, the extension of the mode away from the cylinders is roughly controlled by

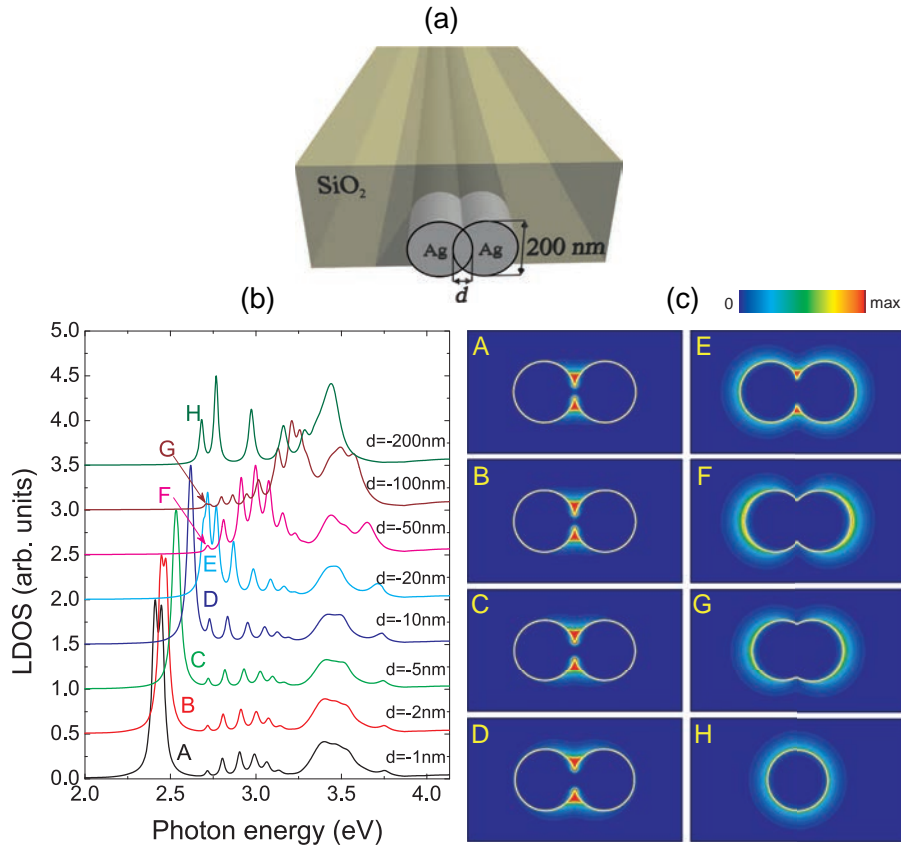


Fig. 2. Gap plasmons of aligned silver nanowires in silica: overlapping configuration. See Fig. 1 for further details and parameters. The LDOS in (b) is calculated 10 nm outside the neck of the dimer profile. The field plots in (c) correspond to the lowest-energy modes labeled in (b).

the wave vector component along the direction perpendicular to the wires, $k_{\perp} = i\sqrt{k_{\parallel}^2 - k_{\text{silica}}^2}$. The mode decays exponentially along that direction, so its extension is limited to a distance $\sim 1/k_{\perp}$. Obviously, this distance decreases with increasing k_{\parallel} , and thus, the migration of the gap mode away from the light cone as the separation between non-touching wires is reduced is accompanied by larger confinement, in agreement with the LDOS spatial distributions of Fig. 1(c). For touching wires, the junction mode seems to be rather unaffected by the actual value of the separation d for $|d| < 10$ nm, thus resulting in nearly identical dispersion diagrams in Fig. 3(i)-3(l).

3. Gap phonon polaritons in aligned alkali-halide microwires

Optical-phonon polaritons in alkali-halide wire pairs can also produce gap modes, as shown in Fig. 4. In particular, the polaritonic resonance in KCl leads to a dielectric function with a Lorentzian profile, encompassing a region of negative real part that mimics the optical behavior of metals (Fig. 4(b)). Rather than gap plasmons, we find gap phonon polaritons. The dispersion diagrams in Fig. 4(c)-4(e) show a new mode emerging within that metallic region (lower mode

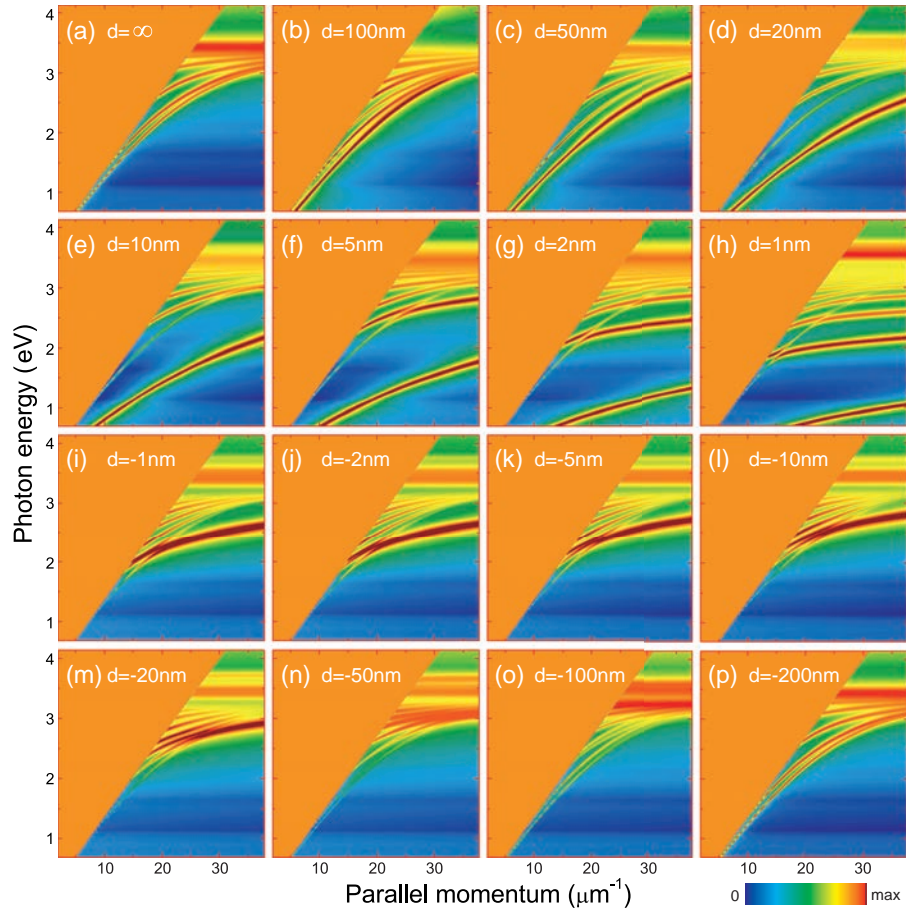


Fig. 3. Gap plasmons of non-touching (a)-(h) and overlapping (i)-(p) aligned silver nanowire pairs embedded in silica. The gap distance d is shown by labels, and $d < 0$ corresponds to the touching configuration. The dispersion diagrams show the LDOS outside the silica light cone at the gap center in (a)-(h) and at a point situated 10 nm outside the dimer neck in (i)-(p).

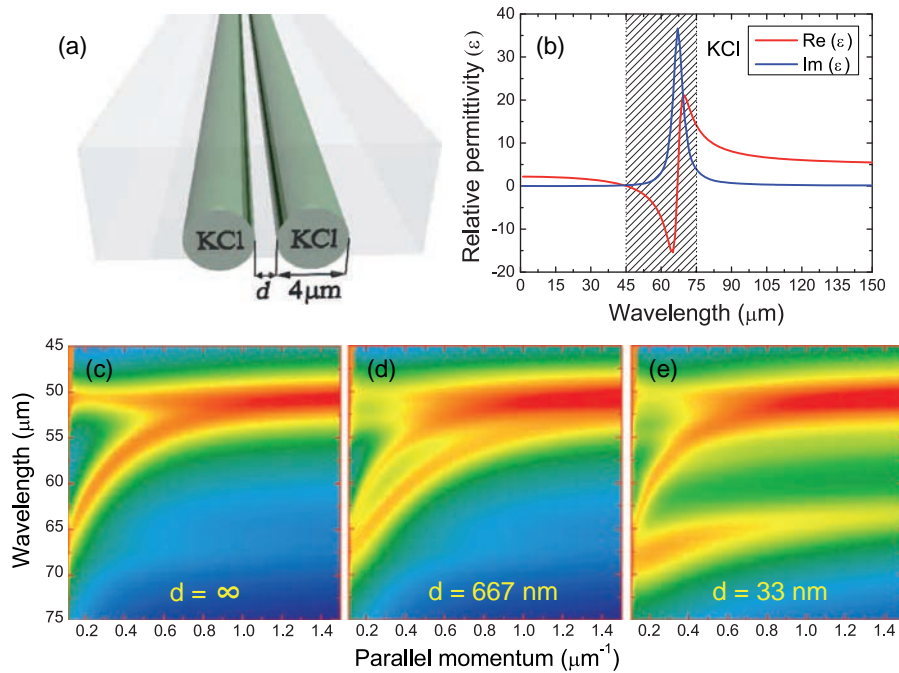


Fig. 4. Gap phonon polaritons in self-standing KCl microwire pairs. **(a)** Schematic view of the geometry. The wire diameter is $4\mu\text{m}$. **(b)** Dielectric function of KCl. **(c)–(e)** Dispersion diagrams showing the total density of photonic states as a function of wave vector parallel to the wires (horizontal axis) and light wavelength (vertical axis) over the spectral region indicated by the shaded area of **(b)**. Different gap distances d are considered, as shown by labels.

in Fig. 4(d)). At very small separations (see Fig. 4(e), in which the distance d is less than 1% of the wire diameter), the mode is pushed towards longer wavelengths. However, in contrast to the metal nanowires, this redshift cannot occur indefinitely because the material changes from metallic (negative permittivity) to dielectric (positive permittivity) at $\sim 70\mu\text{m}$ wavelength. Additionally, losses take off in that region (see imaginary part of the permittivity), the result of which is a significant broadening of the gap mode at short separations (Fig. 4(e)).

We consider in Fig. 5 a structure corresponding to a real dielectric composite consisting of LiF wires embedded in a NaCl matrix [23]. We focus on the phonon polaritons of LiF within the $15 - 45\mu\text{m}$ wavelength range. NaCl behaves as a dielectric over this region (see Fig. 5(b)). As in the KCl wires considered above, the dispersion diagrams for this new structure are showing a gap phonon polariton that builds up when the wires are approached (Fig. 5(d)). Eventually, this mode is broadened and pushed towards the metal-dielectric transition barrier ($\sim 33\mu\text{m}$ wavelength) at short separations (Fig. 5(e)). Incidentally, a guided mode is observed in the spectral region above $50\mu\text{m}$ (not shown), basically consisting of a positive-permittivity LiF waveguide surrounded by a negative-permittivity NaCl matrix, which prevents any significant interaction between waveguides.

Finally, we consider an actual eutectic fabricated by mixing a volume fraction of 24% LiF and 76% NaCl. This leads to the formation of nearly aligned LiF circular microwires in a NaCl matrix, as shown in the micrograph of Fig. 6(a). The local order of the structure is a hexagonal

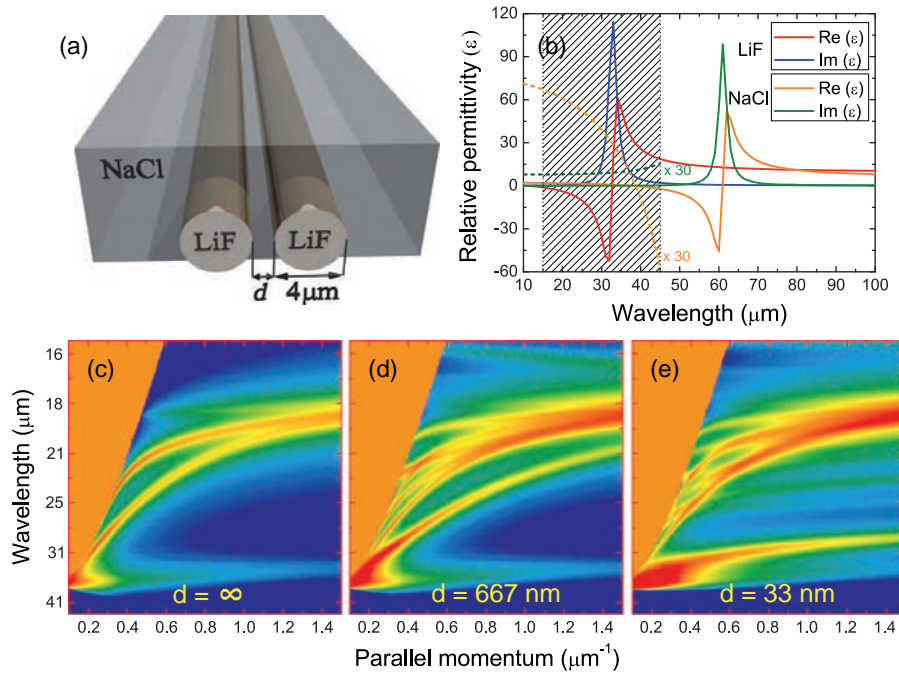


Fig. 5. Same as Fig. 4 for LiF microwires in NaCl. Panel (b) compares the dielectric functions of these two materials within the polaritonic range of interest. The permittivity of NaCl is also shown multiplied by a factor of 30 (dashed curves).

lattice. We analyze the guided modes of this material by considering finite hexagonal arrangements of 1, 7, and 19 microwires of the same diameter and average separation as in the actual eutectic. The resulting dispersion diagrams are shown in Fig. 6(b)-6(d). Interestingly, there is not much variation in the dispersion relation of the lowest-energy mode in these structures: it has a similar dispersion relation in all three finite arrangements. This indicates that the interaction between wires plays a minor role in the tightly bound lowest-energy mode for this relatively large separation between wires, in agreement with the conclusions extracted from Fig. 5. However, higher-energy structure is observed in the 7 and 19 wire arrangements in the region close to the light line, where k_{\perp} is smaller and confinement is lower (see above), so that the modes extend further beyond the individual wires, reaching out neighboring wires and producing mode mixing and energy splittings.

4. Conclusions

In summary, we have shown that gap plasmons in silver nanowires and gap phonon polaritons in LiF microwires exhibit a similar behavior in their respective spectral regions (visible and near-infrared for the plasmons and mid-infrared for the phonon polaritons). A gap mode is formed in the region in between two aligned wires, along which the mode can propagate a long distance. The gap plasmon of non-touching wires migrates towards the red as the gap distance is decreased. In contrast, touching wires support a mode near the junction which is relatively insensitive to the degree of overlap. This configures a singular transition from touching to non-touching, which unlike the case of nanoparticles [21], is not accompanied by a mode becoming physical right at touching (i.e., the gap plasmon is already involving monopoles of opposite

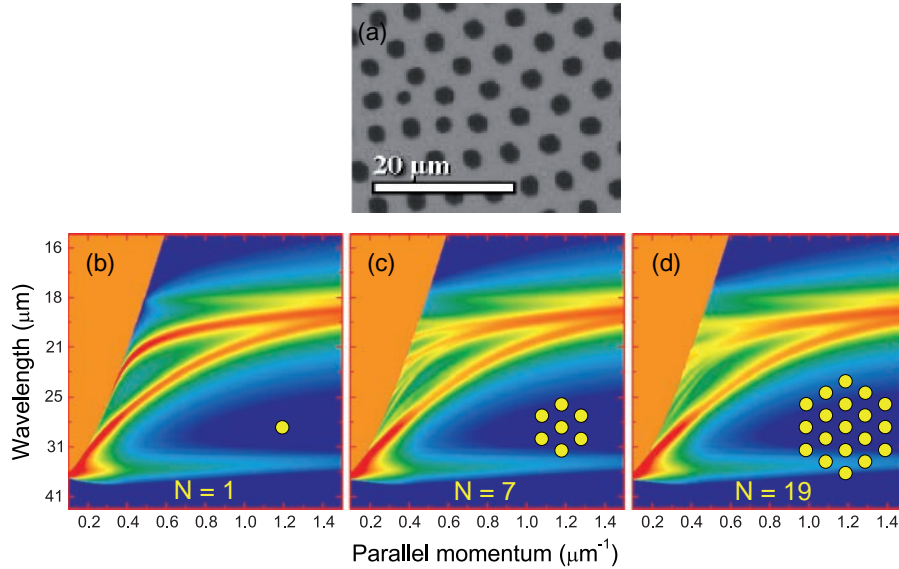


Fig. 6. Polaritonic modes in aligned LiF microwires arranged in a hexagonal lattice inside NaCl. **(a)** Cross section of a fabricated eutectic showing this type of arrangement for wires of $3.3\mu\text{m}$ in diameter and a volume fraction of LiF ≈ 0.24 . **(b)-(d)** Dispersion diagrams showing the total density of photonic states outside the NaCl light cone as a function of wave vector parallel to the wires (horizontal axis) and light wavelength (vertical axis) over the wavelength region corresponding to the shaded area of Fig. 5(b) for finite arrangements of close-packed aligned nanowires consisting of $N = 1$, 7 , and 19 wires, respectively (see insets).

signs in the wires, which are possible due to charge conservation along the propagation direction for finite k_{\parallel} ; this possibility is obviously unphysical in non-touching finite particles). The alkali-halide eutectics under discussion display very little crosstalk between neighboring LiF microwires, and therefore, they could serve as materials on which to funnel an image, which should be preserved between near and far sides of a eutectic slide cut with its surfaces perpendicular to the wires, similar to the so-called endoscope metamaterials [24]. Finally, let us mention that alkali-halide microwire pairs as those considered here could be actually fabricated by manipulation of single-crystal microrods of alkali halides produced by directional solidification (such as LiF, once the NaCl matrix is etched off). Additionally, bunches of separate single-crystal dielectric microwires can be obtained by removing the matrix in some fibrous eutectic systems [23]. The present analysis is thus calling for an experimental implementation based on these methods.

Acknowledgments

We acknowledge support from the European Commission (NMP4-SL-2008-213669-ENSEMBLE), the Spanish MICINN (MAT2010-14885 and Consolider NanoLight.es), and Ibercivis.es. V.M. acknowledges financial support through JAE from CSIC. A.M. acknowledges financial support through FPU from ME. A.S. and D.A.P. thank the Project operated within the Foundation for Polish Science Team Programme co-financed by the EU European Regional Development Fund. A.S. acknowledges COST Action MP0702 for an STSM.